

## Kinetic Model Study of Dry Reforming of Methane Using Cold Plasma

S.M. Fazeli<sup>a</sup>, F. Ravari<sup>a,\*</sup>, H.R. Bozorgzadeh<sup>b</sup> and J. Sadeghzadeh Ahari<sup>c</sup>

<sup>a</sup>Department of Chemistry, Payame Noor University, P.O. Box: 19395-3697, Tehran, Iran

<sup>b</sup>Department of Catalyst, Research Institute of Petroleum Industry (RIPI), P.O. Box: 14665-1998, Tehran, Iran

<sup>c</sup>Research Institute of Petroleum Industry (RIPI), Gas Research Division, P.O. Box: 14665-137, Tehran, Iran

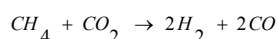
(Received 27 November 2016, Accepted 11 February 2017)

The plasma dry reforming of methane (PDRM) was studied using corona and glow discharge reactors at room temperature. The chemical kinetic model was developed to describe the experimental behavior observed. The kinetic model is proposed based on the assumption that the reactant molecules CH<sub>4</sub> or CO<sub>2</sub> are attacked by active species produced by the plasma discharges, and the production of this active species are function of the plasma power. The modeling allows to foresee the reactants conversion (CH<sub>4</sub> and CO<sub>2</sub>) according to the energy transferred to the gas ( $P \times \tau$ ), while considering the argon dilution value in the feed gas. The  $\beta$  value was characteristic of the energy cost; the lower  $\beta$  value indicated better efficiency. The  $\beta$  value of CH<sub>4</sub> was found to be 10.42 and 9.91 J and for CO<sub>2</sub> equal to 12.24 and 15.42 J for corona and glow discharge plasma, respectively. This result is in accordance with the higher dissociation energy of CO<sub>2</sub> compared to CH<sub>4</sub>.

**Keywords:** Methane, Kinetic model, plasma, Synthesis gas

### INTRODUCTION

In recent years, about 85% of energy consumption is obtained from fossil fuels (such as coal, crude oil, and natural gas). Human activities and utilization of fossil resources resulted in emissions of greenhouse gasses (CO<sub>2</sub>, H<sub>2</sub>O) as a result of global warming [1,2]. Hydrogen is a healthy fuel source and considered as an environmentally friendly material in different industries. The conversion of methane to hydrogen, added-value chemicals such as hydrocarbons and methanol to replace fuels attracted a lot of attentions. DRM is production of synthesis gas (hydrogen and carbon monoxide) from CH<sub>4</sub> and CO<sub>2</sub> by the following intensively endothermic reaction:



$$\Delta H = 247 \text{ kJ.mol}^{-1} \quad (1)$$

Thermodynamically, DRM occurs at the temperature > 640 °C. If this reaction takes place at temperatures lower than 800 °C, carbon may produce, meanwhile, carbon deposition is formed from methane decomposition at high temperature [3]. According to the thermodynamic principles, the Gibbs free energy change of DRM reaction ( $\Delta G$ ) is positive, so the reaction is thermodynamically unfavorable [4].

Synthesis gas is an important feedstock for the Fischer-Tropsch reaction to produce methanol, liquid hydrocarbons, etc. The Fischer-Tropsch process is a collection of chemical reactions converting synthesis gas into liquid hydrocarbons [5-7].

Recently, non-thermal plasma reactors introduced one of the newest processes for DRM. The benefits of using the cold plasma reactors consist of: non-equilibrium phase, need to low input power and the capacity to perform gas reactions at low temperatures. Also, this method overcomes the high-temperature problem in the catalytic processes [8]. The DRM processes were investigated for producing

\*Corresponding author. E-mail: fatemeravari@yahoo.com

synthesis gas by using a manifold of plasma sources such as the microwave (MW) discharges [9], dielectric barrier discharges (DBDs) [10], corona discharges [11] and gliding arc discharges (GADs) [12]. In these studies, CO<sub>2</sub> and CH<sub>4</sub> are often introduced into the plasma reactor with a dilution gas like helium or argon [13,14].

Methane plasma reforming and finding optimum conditions were abstruse. Also, the products selectivity's prediction and mechanism of the reaction were a theoretical problem. In recent years, in order to achieve the optimal prediction, describing and solving this problem, kinetic models and mathematical modeling were used [15-18]. In the plasma-assisted methane coupling reactions such as CO<sub>2</sub> reforming and partial oxidation reactions, studied poorly referred to reaction mechanisms and kinetic models.

In this research, the PDRM is studied for the two types of cold plasma reactors (corona and glow discharge) and then the results of PDRM are compared with other non-thermal plasmas. Also, the kinetic model is developed to estimate the real perspectives of PDRM in the plasma field.

## EXPERIMENTAL

In this study, to produce synthesis gas from methane and carbon dioxide at atmospheric pressure the corona and glow discharge plasma were used. Figure 1 depicts the experimental setup and schematic of the plasma reactors.

The corona discharge plasma tubular microreactor consisted of a wire-plate tungsten electrode configuration. The reactor vertically oriented, with the gas flow from top to bottom. The upper electrode was a tungsten wire suspended and centered axially within the reactor tube. A dc power supply was used with a high-voltage transformer of 0-12 kV to initiate corona discharges. An oscilloscope (Tektronix TDS2024B) measured the typical breakdown voltage (about 5-6 kV), and the discharge power. The corona's current was in the range of 0.5-5 mA (Fig. 1b). The outer diameter of the reactor is 30 mm, the length of the reactor is 50 mm.

The glow discharge plasma reactor consists of two tungsten electrodes located inside the hourglass shaped quartz tube with inner diameter 7 mm top and bottom and 2 mm in the middle (Fig. 1c). The special design for plasma

reactor lead all feed gasses to cross from plasma region. The reactor was oriented vertically, with the gas flow from top to bottom. The upper electrode was needle-shaped and connected to a high voltage, it was at the positive potential as the anode and the diameter of it was 2 mm. The plate electrode was grounded as the cathode and its potential is 0 (V). Ionized gasses were generated between these electrodes inside the quartz tube. The outer diameter of the reactor is 40 mm and the length of the reactor is 100 mm.

The mass flow controllers (Brooks 5850TR) controlled the flow rates of the two ultra pure reactants, CH<sub>4</sub> (>99.99%) and CO<sub>2</sub> (>99.5%) in a molar ratio of CH<sub>4</sub>/CO<sub>2</sub> = 1/2 and 3, with 60% argon as a diluting gas, for corona and glow discharge plasma reactor set up. The reactants were well-mixed and flowed through the reactor at room temperature and atmospheric pressure. However, the temperatures of the reactants increased as they passed through the plasma area as a result of the conversion of electric energy into heat energy. Under each set of conditions, for stabilization before product analysis allowed 60 min

Two condensers introduced the exhaust gas from the reactors, cooled by a mixture of water and ice to remove the formed water and liquid organic products such as alcohols. The compositions of the feed gas mixture and the outlet gas were quantitatively measured by an online gas chromatograph (Agilent 6890N) equipped with a thermal conductivity (TCD) and a flame ionization detector (FID). The flow rates of the inlet and outlet gas were also measured by a soap-bubble flow meter to carry out balance calculations of the elements.

The experimental setup sections and their function are shown in Table 1 [11]. Methane and carbon dioxide conversion are defined as follows:

$$\text{CH}_4\text{Conversion (\%)} = X_{\text{CH}_4} = \frac{\text{moles of CH}_4\text{ converted}}{\text{moles of CH}_4\text{ introduced}} \times 100 \quad (2)$$

$$\text{CO}_2\text{Conversion (\%)} = X_{\text{CO}_2} = \frac{\text{moles of CO}_2\text{ converted}}{\text{moles of CO}_2\text{ introduced}} \times 100 \quad (3)$$

The following relation is applied for calculation of selectivity and yield of products:

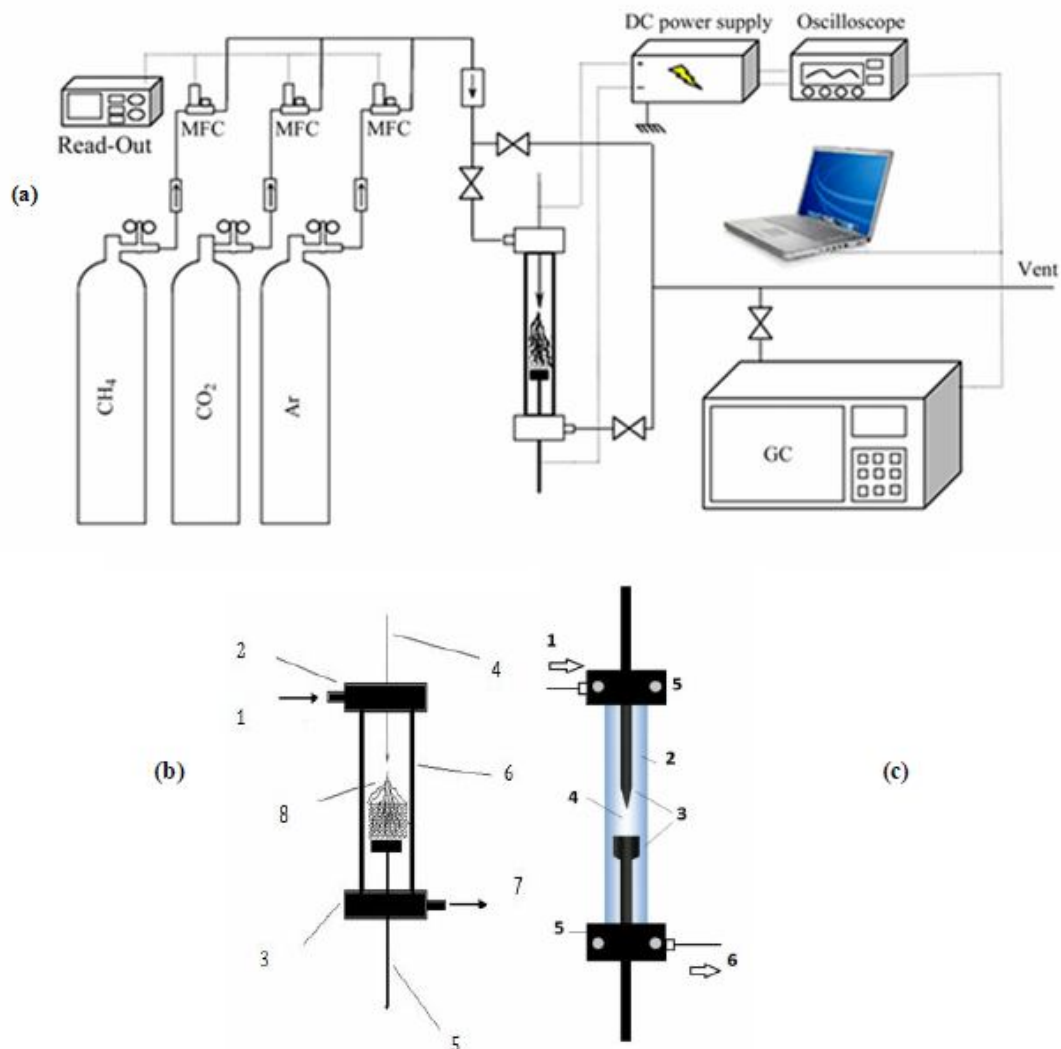


**Fig. 1.** (a) Schematic diagram of the experimental set-up. (b) Corona discharge plasma reactor: 1. feed gas inlet, 2, 3. Teflon holder, 4, 5. tungsten electrode, 6. quartz tube, 7. gas outlet, 8. discharge region [11] (c) Glow discharge plasma reactor: 1. feed gas inlet, 2. quartz tube, 3. tungsten electrode, 4. discharge region, 5. Teflon holder, 6. gas outlet.

$$SH_2 (\%) = \frac{\text{moles of } H_2 \text{ produced}}{2 \times \text{moles of } CH_4 \text{ consumed}} \times 100 \quad (4)$$

$$SCO (\%) = \frac{\text{moles of } CO \text{ produced}}{\text{moles of } CH_4 \text{ consumed} + \text{moles of } CO_2 \text{ consumed}} \times 100 \quad (5)$$

$$\text{Yield } H_2 (\%) = SH_2 (\%) \times X_{CH_4} (\%) \quad (6)$$

## RESULTS AND DISCUSSION

### Influence of Dilution by Argon on Energy Deposit

The dilution by argon varied from 20-60% while the molar ratio  $CH_4/CO_2$  was kept constant. The deposited energy was measured at 12 kV. The energy deposit per pulse increased significantly as the dilution by argon increased, whatever the applied voltage. This phenomenon is due to the physico-chemical modification of the

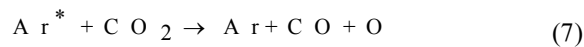
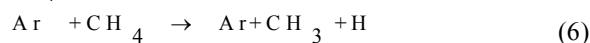
**Table 1.** Experimental Data Ranges Used in this Study for Development of Chemical Kinetic Model [11]

Types of plasma: Corona discharge						
Feed flow rate (ml min <sup>-1</sup> )	Power	XCH <sub>4</sub> %	XCO <sub>2</sub> %	SH <sub>2</sub> %	SCO%	YH <sub>2</sub> %
CO <sub>2</sub> /CH <sub>4</sub> ratio = 0.5	(w)					
50	4	35	24	61	73	21
100	4	28	20	63	76	17
150	4	25	17	64	70	16
200	4	22	15	65	69	14
250	4	17	13	66	70	11
100	4	25	18	72	75	18
100	6	43	30	67	76	29
100	10	62	43	65	80	40
Types of plasma: Glow discharge						
Feed flow rate (ml min <sup>-1</sup> )	Electrode gap	XCH <sub>4</sub> %	XCO <sub>2</sub> %	SH <sub>2</sub> %	SCO%	YH <sub>2</sub> %
CO <sub>2</sub> /CH <sub>4</sub> ratio = 3, voltage (kV) = 10	(mm)					
60	20	75	21	30	70	22
97	20	50	15	38	47	19
145	20	38	12	19	26	7
60	25	56	37	47	55	26
97	25	55	27	31	49	17
145	25	51	16	27	36	14
Power (w)						
Feed flow rate (ml min <sup>-1</sup> ) = 100, Electrode gap (mm) = 20	XCH <sub>4</sub> %	XCO <sub>2</sub> %	SH <sub>2</sub> %	SCO%	YH <sub>2</sub> %	
10	73	21	30	70	22	
12	78	27	29	63	23	
14	85	37	28	50	23.5	
16	89	46	27	36	24	

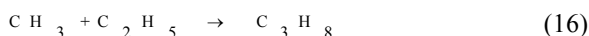
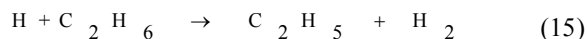
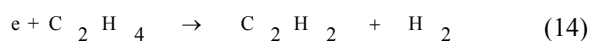
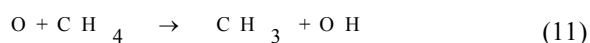
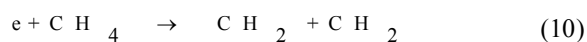
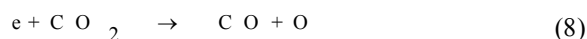
plasmagen gas resulting from the presence of the dilution gas: argon. The argon such as helium leads to a lower breakdown voltage leading to a higher energy deposit [19].

### Conversion, Reactivity, and Selectivity

The higher reactivity of reactants molecules (CH<sub>4</sub> and CO<sub>2</sub>) in the presence of argon is explained by the ‘‘Penning ionization’’ phenomenon, which corresponds to an energy transfer from the excited atom or molecule to other atom or molecule in ground state [20-22]. In this case, the energy transfers proceed from metastable argon (Ar\*) to the reactant molecules (CH<sub>4</sub> and CO<sub>2</sub>). Whatever the CH<sub>4</sub>/Ar mole ratio decreased, the CH<sub>4</sub> conversion increased significantly. The reactant dissociation is shown as Eqs. (6) and (7) [23,24]:



The results can be explained by the mechanisms of the reactions involved, indeed H<sub>2</sub> and CO are formed directly from CH<sub>4</sub> and CO<sub>2</sub> while the formation of other hydrocarbons (C<sub>2</sub> and C<sub>3</sub>) requires the recombination of methyl radicals according to the following reactions:



As soon as the reactive species (methyl radicals) are diluted with argon, the probability of the collision of radicals decreases, consequently the selectivities for higher hydrocarbons decreases as the dilution factor increases.

The CH<sub>4</sub> (XCH<sub>4</sub>) and CO<sub>2</sub> (XCO<sub>2</sub>) conversion significantly decrease when the feed flow rate increases, which can be attributed to a decrease of the residence time of the methane and carbon dioxide in the discharge volume, resulting in a reduced chance for reactant molecules (CH<sub>4</sub> and CO<sub>2</sub>) to collide with energetic electrons (e) and reactive species (Ar\* and CH<sub>3</sub>) (Fig. 2).

The discharge power is an effective factor for the plasma processing of methane. In corona plasma, the conversion of CH<sub>4</sub> and yield of hydrogen almost linearly increase with the increase of discharge power for 10 W that is reaching to 62% at 10 W. The maximum yield of hydrogen is 40 % for corona discharge plasma. In addition, CO selectivity increases from 75 to 80%. The C<sub>2</sub> hydrocarbons produced from Eqs. (12)-(14) in plasma phase, these hydrocarbons broken again, so producing CO molecule probability increased. Meanwhile, hydrogen reacts with oxygen atoms (Eq. (8)) and H<sub>2</sub>O is produced, thus H<sub>2</sub> selectivity decreases to 65% from 4 to 10 W.

In glow discharge plasma, conversion of CH<sub>4</sub> increases with the increase of discharge power for 16 W. Thus, the CH<sub>4</sub> conversion increases from 73 to 89%. The maximum yield of hydrogen is 26% for glow discharge plasma. Figure 3 shows the conversion of CH<sub>4</sub> and CO<sub>2</sub> for the two plasma reactors at different input plasma powers.

Table 1 summarized the overall range of the operating condition used in this study for developing the chemical kinetic models.

### Comparison of DRM Among Different Non-thermal Plasmas

Table 2 presents interesting results when comparing the DRM by different typical plasmas. XCH<sub>4</sub>, XCO<sub>2</sub>, SH<sub>2</sub> and SCO were applied for prediction of the methane reforming performance. Our plasmas show a good result.

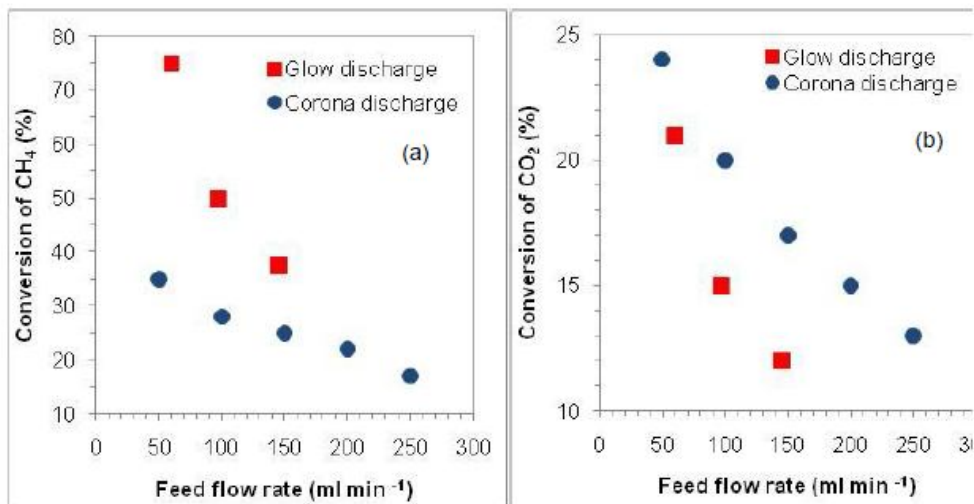


**Fig. 2.** Effect of feed flow rate on (a) CH<sub>4</sub> and (b) CO<sub>2</sub> conversions in corona and glow discharge plasma ((Ar = 60 % dilution, CH<sub>4</sub>/CO<sub>2</sub> = 0.5, 3 power = 4, 10 W; respectively).

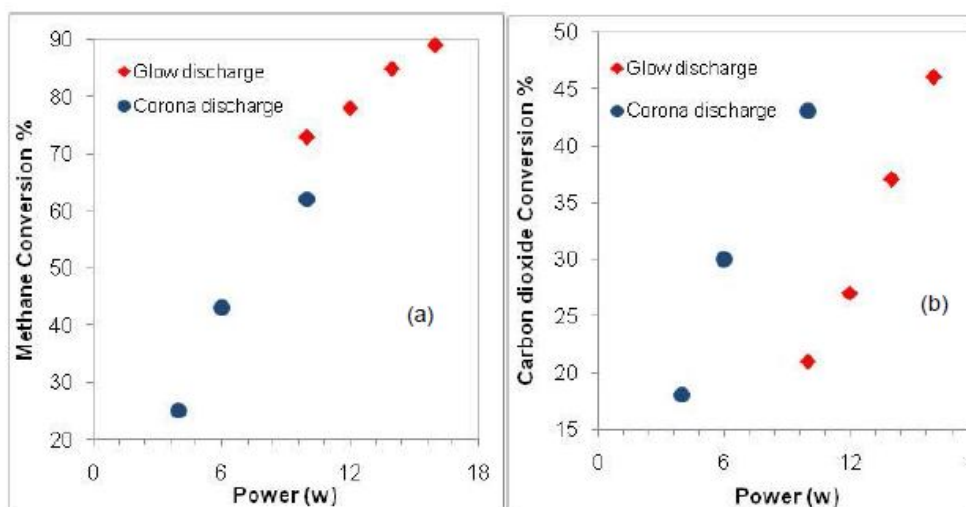


**Fig. 3.** Effect of input plasma power on (a) CH<sub>4</sub> and (b) CO<sub>2</sub> conversion in corona and glow discharge plasma ((Ar = 60 % dilution, CH<sub>4</sub>/CO<sub>2</sub> = 0.5, 3 feed flow rate=100 ml/min; respectively).

### A Global Chemical Kinetic Model

A simplified global kinetic model can describe the experimental behavior observed by changing the argon dilution factor. The two reactors used in this experiment were compared with a global kinetic model to describe the DRM reaction behavior. In different plasma reactors such as corona and DBD in the field of methane and other

hydrocarbons conversion used this model [25,26,32-35]. The free radical processes are the main mechanisms in non-equilibrium plasma reaction [7,33,36].

The model steps were:

1. The active species (R) such as radicals and Ar active species produced by plasma discharges attacked to methane or carbon monoxide molecules (S):

**Table 2.** Comparison of Conversion in Different Plasmas

Plasma	Feed flow rate (ml min <sup>-1</sup> )	CO <sub>2</sub> /CH <sub>4</sub>	P (W)	Conversion		Selectivity		Refs.
				(%)		(%)		
				CH <sub>4</sub>	CO <sub>2</sub>	H <sub>2</sub>	CO	
Corona	43	1/1	46.3	62.4	47.8	70	66.8	[27]
DBD	150	2/1	500	64.3	55.4	-	33.3	[28]
Glow discharge	120	1/1	23	61	50	77.5	63	[29]
Plasma jet	0.83	4/6	770	45.6	34	78.1	85.4	[30]
GAD	1000	1/1	190	40	31	50	62	[26]
Thermal plasma	2.17 × 10 <sup>4</sup>	4/6	8.5 × 10 <sup>3</sup>	78.9	84.3	43.48	82.2	[31]
DBD	45	1/1	180	27.5	23.8	50.3	57.5	[25]
Corona discharge	100	2/1	10	62	43	65	80	This paper
Glow discharge	60	1/3	16	89	47	30	70	This paper

S + R → products

2. The reaction rate was:  $r = k_1 R.S$ ,

where,  $k_1$  is the reaction rate constant, R is the radical concentration, and S is the reactant concentration.

3. The plasma input power and production rate of R was commensurate:  $r_R \times P$

where,  $r_R$  is the production rate of radicals per power supplied.

The Eqs. of (8) and (9) were mass conservation of the reactant molecules (S) and radicals (R) [25]:

$$\frac{dS}{dt} = -k_1.R.S \quad (17)$$

$$\frac{dR}{dt} = r_R \times P - k_2.R - k_1.R.S_0 \quad (18)$$

where,  $k_2$  represents the reaction rate constant of the R loss, P the input power and  $S_0$  the reactant (CH<sub>4</sub> + CO<sub>2</sub>) initial concentration.

By application of the stationary state principle and if we expect that the plasma discharges are reproducible, the

concentration of radicals is constant along the reactor [25]. Thus,

$$\frac{dR}{dt} = 0$$

and

$$R = \frac{r_R \times P}{k_2 + k_1 R.S_0} \quad (19)$$

$$\frac{dS}{dt} = -k_1 S \frac{r_R \times P}{k_2 + k_1 R.S_0} \quad (20)$$

After integration from  $t = 0$  (reactor inlet) to  $\tau$  = s (reactor outlet):

$$\frac{S}{S_0} = \exp\left(-\frac{k_1 r_R \times P \times \tau}{k_2 + k_1 S_0}\right) \quad (21)$$

or

$$\ln(1 - X) = \left(-\frac{P \times \tau}{\beta(S_0)}\right) \quad (22)$$

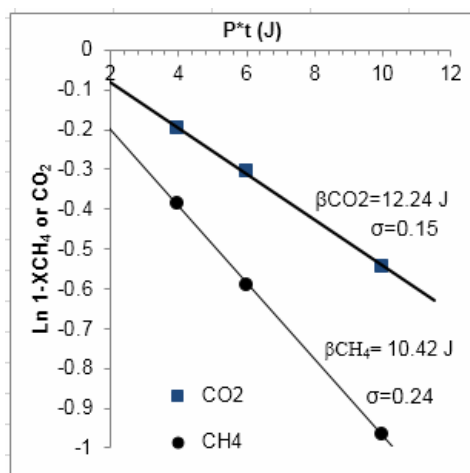


**Fig. 4.** Estimated  $\beta$  value for  $\text{CH}_4$  and  $\text{CO}_2$  with  $X_0 = 0.4$  (Ar = 60% dilution) for corona discharge plasma according to the kinetic model ( $\sigma$ : standard deviation).

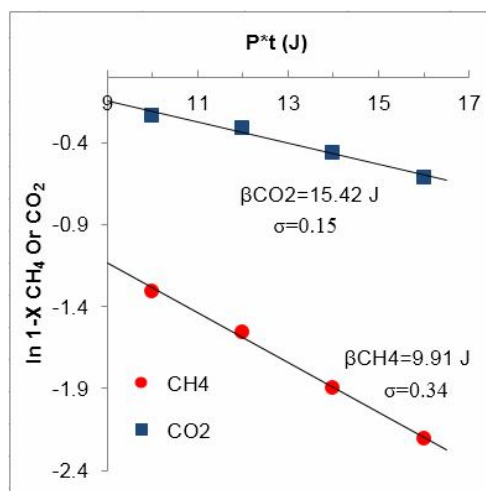


**Fig. 5.** Estimated  $\beta$  value for  $\text{CH}_4$  and  $\text{CO}_2$  with  $X_0 = 0.25$  (Ar = 60% dilution) for glow discharge plasma according to the kinetic model ( $\sigma$ : standard deviation).

if

$$\beta(S_0) = \frac{1}{r_R} \left( \frac{k_2}{k_1} + S_0 \right) \quad (23)$$

$$X = 1 - \exp\left(-\frac{P \times \tau}{\beta(S_0)}\right)$$

or

$$\ln(1 - X) = \left(-\frac{P \times \tau}{\beta(S_0)}\right) \quad (24)$$

There is an exponential function of the  $\text{CH}_4$  and  $\text{CO}_2$  conversion and product. A linear function between the initial reactant concentration and the production rate of radicals represents  $\beta$  factor. Figures 4 and 5 present the  $\beta$

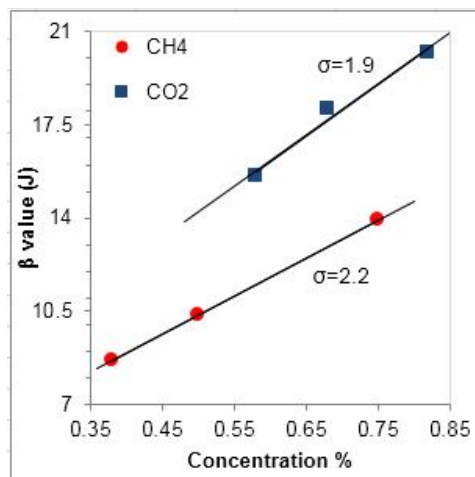


**Fig. 6.** The  $\beta$  value according to the CH<sub>4</sub> and CO<sub>2</sub> concentrations for corona discharge plasma ( $\sigma$ : standard deviation).

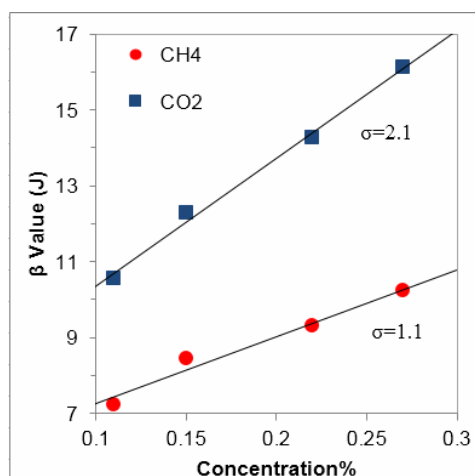


**Fig. 7.** The  $\beta$  value according to the CH<sub>4</sub> and CO<sub>2</sub> concentrations for glow discharge plasma ( $\sigma$ : standard deviation).

values evaluated with the CH<sub>4</sub> and CO<sub>2</sub> concentrations. In this study, the  $\beta$  value for CH<sub>4</sub> and CO<sub>2</sub> are equal to 10.42 and 12.24 J for corona discharge plasma, and to 9.91 and 15.42 J for glow discharge plasma respectively, because of the higher dissociation energy of CO<sub>2</sub> compared to CH<sub>4</sub>.

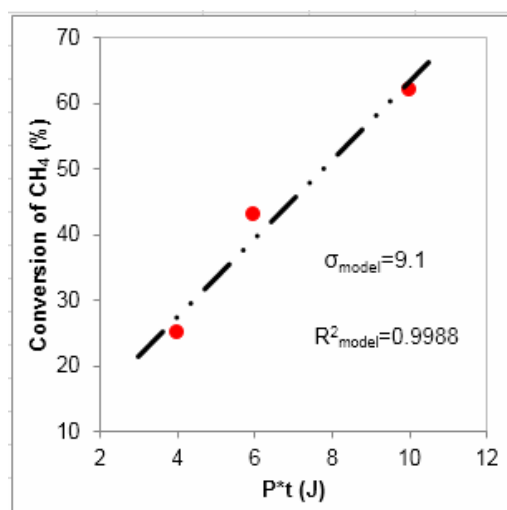
The evolution of  $\beta$  values with the CH<sub>4</sub> and CO<sub>2</sub> concentrations are presented in Figs. 6 and 7. A linear increase of  $\beta$  with increasing the concentration of CH<sub>4</sub> and CO<sub>2</sub> are observed. The  $\beta$  value is characteristic of the

energy cost. In the literature, the lower  $\beta$  value indicated better efficiency [36-38].

Table 3 shows the obtained values of  $r_R$  and  $k_2/k_1$  for CH<sub>4</sub> and CO<sub>2</sub>. It shows that the production rate of radicals depends strongly on the reactant. The  $k_2/k_1$  ratio value indicated the dominate reaction; the reaction between active species and reactant driving to product formation, or the active species loss reaction by recombination or desexcitation [25].

**Table 3.** Kinetic Modeling Parameters

Reactant	Linearity	$K_2/k_1$	$\Gamma_R$ (ppm J <sup>-1</sup> )
Corona			
CH <sub>4</sub>	$(\beta(S_0)) = 14.29S_0 + 4.70$	0.33	69979
CO <sub>2</sub>	$(\beta(S_0)) = 19.15S_0 + 4.58$	0.24	52219
Glow discharge			
CH <sub>4</sub>	$(\beta(S_0)) = 17.60S_0 + 5.51$	0.31	56818
CO <sub>2</sub>	$(\beta(S_0)) = 33.70S_0 + 6.99$	0.21	29673

**Fig. 8.** The simulated behavior of CH<sub>4</sub> conversion according to energy transferred to the gas during corona plasma discharge:  $P \times \tau$  (J) (●, ■: experimental, - - - calculated data and  $\sigma$ : standard deviation).

In corona and glow discharge plasma, for CO<sub>2</sub>, the value of the  $k_2/k_1$  ratio (0.24, 0.21) respectively; indicates that the active species reactions are favored compared to their loss. For CH<sub>4</sub> ( $k_2/k_1$  ratio: 0.33, 0.31) respectively, the radicals are lost in the reaction, also those emanated from CH<sub>4</sub> recombination occurs more than from CO<sub>2</sub> [25]. The following equation calculated the  $\beta$  values:

$$X = 1 - \exp\left(\frac{P \times \tau}{\beta(S_0)}\right)$$

As shown in Figs. 8-11, this modeling is fitted well with the experimental data of CH<sub>4</sub> and CO<sub>2</sub> conversions in the presence of plasma discharges. Based on this simple kinetic model, there is an authentic correlation between the CH<sub>4</sub> and CO<sub>2</sub> conversions and energy transferred to the gas during plasma discharge ( $P \times \tau$ ).

## CONCLUSIONS

The PDRM was investigated in the corona and glow

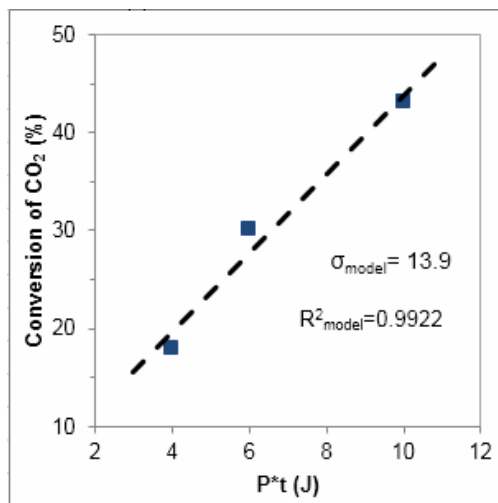


**Fig. 9.** The simulated behavior of CO<sub>2</sub> conversion according to energy transferred to the gas during corona plasma discharge:  $P \times \tau$  (J) (●, ■: experimental, - - - calculated data and  $\sigma$ : standard deviation).

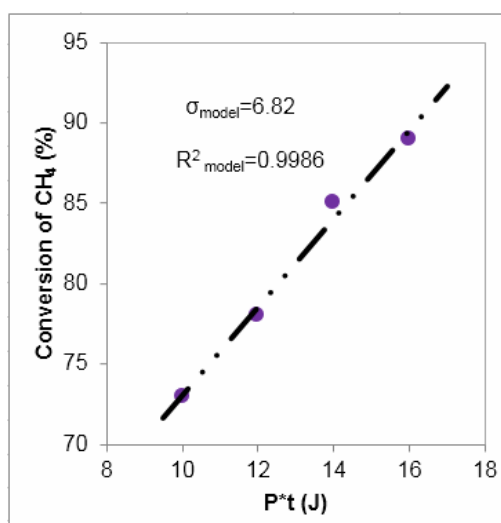


**Fig. 10.** The simulated behavior of CH<sub>4</sub> conversion according to energy transferred to the gas during glow plasma discharge:  $P \times \tau$  (J) (●, ■: experimental, - - - calculated data and  $\sigma$ : standard deviation).

discharge reactors at atmospheric pressure and room temperature. The chemical kinetic model was developed to describe the experimental behavior observed. The kinetic model is proposed based on the assumption that the reactant molecules CH<sub>4</sub> or CO<sub>2</sub> are attacked by active species

produced by the plasma discharges, and the production of this active species are function of the plasma power. The modeling allows to foresee the reactant conversion (CH<sub>4</sub> and CO<sub>2</sub>) according to the energy transfer to the gas ( $P \times \tau$ ), but the model consider also the argon dilution value in the

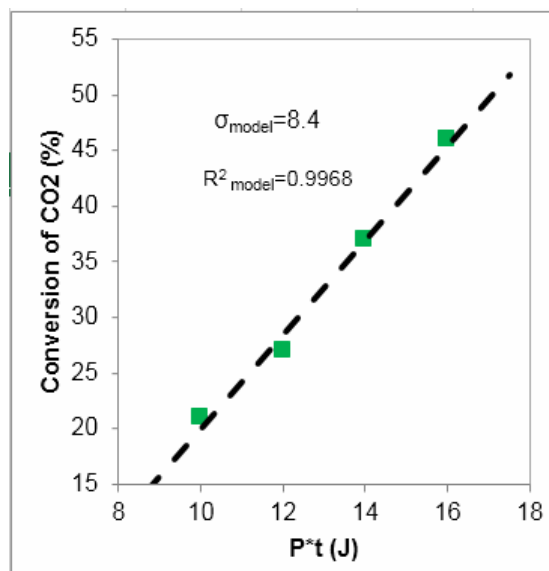


**Fig. 11.** The simulated behavior of CO<sub>2</sub> conversion according to energy transferred to the gas during glow plasma discharge:  $P \times \tau$  (J) (●, ■: experimental, - - - calculated data and  $\sigma$ : standard deviation).

feed gas. The  $\beta$  value was characteristic of the energy cost, the lower  $\beta$  value indicated better efficiency. The  $\beta$  value of CH<sub>4</sub> was found to be 10.42 and 9.91 J and for CO<sub>2</sub> is equal to 12.24 and 15.42 J for corona and glow discharge plasma, respectively. This result is in accordance with the higher dissociation energy of CO<sub>2</sub> compared to CH<sub>4</sub>. The experimental data (CH<sub>4</sub> and CO<sub>2</sub> conversion) fits very well with the proposed kinetic law. The kinetic model demonstrated that there is an exponential function of the reactant conversion and plasma energy. This model also represents that a plasma reactor with a smaller CH<sub>4</sub>/CO<sub>2</sub> molar ratio (corona discharge plasma) has a higher energy efficiency for CO<sub>2</sub> and lower for CH<sub>4</sub>.

## REFERENCES

- [1] Shafiee, S.; Topal, E., when will fossil fuel reserves be diminished? *Energy Policy*. **2009**, *37*, 181-189, DOI: 10.1016/j.enpol.2008.08.016.
- [2] Samimi, A.; Zarinabadi, S., Reduction of Greenhouse gases emission and effect on environment. *Australian J Basic and Applied Sci.* **2011**, *5*, 752-756.
- [3] Fidalgo, B.; Menendez, J., Carbon materials as catalysts for decomposition and CO<sub>2</sub> reforming of methane: A review. *Chinese Journal of Catalysis*. **2011**, *32*, 207-216, DOI: 10.1016/S1872-2067(10)60166-0.
- [4] Smith, J. M.; Van Ness, H. C.; Abbott, M. M., *Introduction to chemical engineering thermodynamics*, 7th ed. Mc Graw-Hill Book Company, New York: **2005**; p. 350.
- [5] Arsalanfar, M.; Mirzaei, A. A.; Atashi, H.; Bozorgzadeh, H. R.; Vahid, S.; Zare, A., An investigation of the kinetics and mechanism of Fischer-Tropsch synthesis on Fe-Co-Mn supported catalyst. *Fuel Processing Technology*. **2012**, *96*, 150-159, DOI: 10.1016/j.fuproc.2011.12.018.
- [6] Reubroycharoen, P.; Vitidsant, T.; Yoneyama, Y.; Tsubaki, N., Development of a new low-temperature methanol synthesis process. *CatalToday*, **2004**, *89*: 447-454, DOI: 10.1016/j.cattod.2004.01.006.
- [7] Li, M. W.; Xu, G.; Tian, Y.; Chen, L.; Fu, H., Carbon dioxide reforming of methane using DC corona discharge plasma reaction *J. Phys. Chem. A*, **2004**, *108*, 1687-1693, DOI: 10.1021/jp037008q.
- [8] Fidalgo, B.; Domínguez, A.; Pis, J.; Menéndez, J., Microwave-assisted dry reforming of methane. *Int. J. Hydrogen Energy* **2008**, *33*, 4337-4344, DOI: 10.1016/j.ijhydene.2008.05.056.

- [9] Tao, X. M.; Bai, M. J.; Li, X.; Long, H. L.; Shang, S. Y.; Yin, Y. X.; Dai, X. Y., CH<sub>4</sub>-CO<sub>2</sub> reforming by plasma-challenges and opportunities. *Prog Energy Combust Sci.* **2011**, *37*, 113-124, DOI: 10.1016/j.peccs.2010.05.001.
- [10] Gallon, H. J.; Tu, X.; Whitehead, J. C., Effects of reactor packing materials on H<sub>2</sub> production by CO<sub>2</sub> reforming of CH<sub>4</sub> in a dielectric barrier discharge. *Plasma Process Polym.* **2012**, *9*, 90-97, DOI: 10.1002/ppap.201100130.
- [11] Aziznia, A.; Bozorgzadeh, H. R.; Seyed-Matin, N.; Baghalha, M.; Mohamadizadeh, A., Comparison of dry reforming of methane in low temperature hybrid plasma-catalytic corona with thermal catalytic reactor over Ni/ $\gamma$ -Al<sub>2</sub>O<sub>3</sub>, *J. Nat. Gas Chem.* **2012**, *21*, 466-475, DOI: 10.1016/S1003-9953(11)60392-7.
- [12] Rueangjitt, N.; Sreethawong, T.; Chavadej, S.; Sekiguchi, H., Nonoxidative reforming of methane in a mini-gliding arc discharge reactor: effects of feed methane concentration, feed flow rate, electrode gap distance, residence time, and catalyst distance. *Plasma Chem. Plasma P.* **2011**, *31*, 517-534, DOI: 10.1007/s11090-011-9299-y.
- [13] Liu, C.; Marafee, A.; Allinson, R.; Lobban, L., Methane conversion to higher hydrocarbons in a corona discharge over metal oxide catalysts with OH groups. *Appl Catal A: Gen* **1997**, *164*, 21-33, DOI: 10.1016/S0926-860X(97)00154-3.
- [14] Huang, A.; Xia, G.; Wang, J.; Suib, S. L.; Hayashi, Y.; Matsumoto, H., CO<sub>2</sub> reforming of CH<sub>4</sub> by atmospheric pressure ac discharge plasmas, *J. Catal.* **2000**, *189*, 349-359, DOI: 10.1006/jcat.1999.2684.
- [15] Mousavipour, S. H.; Doroodmand, M. M.; Zarin Hamedani, S. M. A.; Zarei, V.; Dehbozorgi, M. R., Conversion of natural gas into the gaseous constituents and nano-graphene in the presence of chlorine as homogeneous promoter by DC-spark discharge. *J. Iran. Chem. Soc.* **2015**, *12*, 1303-1311. DOI: 10.1007/s13738-015-0595-y.
- [16] De Bie, C.; Verheyde, B.; Marten, T.; van Dijk, J.; Paulussen, S.; Bogaerts, A., Fluid modeling of the conversion of methane into higher hydrocarbons in an atmospheric pressure dielectric barrier discharge. *Plasma Processes Polym.* **2011**, *8*, 1033-1058, DOI: 10.1002/ppap.201100027.
- [17] De Bie, C.; Marten, T.; van Dijk, J.; Paulussen, S.; Verheyde, B.; Corthals, S.; Bogaerts, A., Dielectric barrier discharges used for the conversion of greenhouse gases: modeling the plasma chemistry by fluid simulations. *Plasma Source Sci. Technol.* **2011**, *20*, 024008, DOI: 10.1088/0963-0252/20/2/024008.
- [18] Snoecks, R.; Aerts, R.; Tu, X.; Bogaerts, A., Plasma-based dry reforming: a computational study ranging from the nanoseconds to seconds time scale. *J. Phys. Chem. C* **2013**, *117*, 4957-4970, DOI: 10.1021/jp311912b
- [19] Guaitella, O., PhD thesis, Ecole Polytechnique, Palaiseau, France, **2006**.
- [20] Penning, F. M., Die glimmentladung bei niedrigem druck zwischen koaxialen zylindern in einem axialen magnetfeld. *Physica* **1936**, *3*, 873-894. DOI: 10.1016/S0031-8914(36)80313-9.
- [21] Fridman, A., *In: Plasma chemistry* (ed). Cambridge University Press, Cambridge: **2008**; pp. 21-28.
- [22] Lieberman, M. A.; Lichtenberg, A. J., *In: Principles of plasma discharges and materials processing* (ed). Wiley, (2nd ed): **2005**; pp. 238-245.
- [23] Chapman, B., *Glow discharge processes*. Wiley, New York, **1980**.
- [24] Wang, Y. -F.; Tsai, C. -H.; Shih, M.; Hsieh, L. -T.; Chang, W. -C., Direct conversion of methane into methanol and formaldehyde in an RF plasma environment II: Effects of experimental parameters. *Aerosol and Air Quality Res.* **2005**, *5*, 211-224.
- [25] Goujard, V.; Tatibouet, J. M.; Batiot-Dupeyrat, C., Carbon dioxide reforming of methane using a dielectric barrier discharge reactor: effect of helium dilution and kinetic model. *Plasma Chem Plasma P.* **2011**, *31*, 315-325, DOI: 10.1007/s11090-010-9283-y
- [26] Indarto, A.; Choi, J. -W.; Lee, H.; Song, H. K., Effect of additive gases on methane conversion using gliding arc discharge. *Energy*, **2006**, *31*, 2986-2995, DOI: 10.1016/j.energy.2005.10.034.
- [27] Yang, Y., Methane conversion and reforming by nonthermal plasma on pins. *Ind. Eng. Chem. Res.* **2002**, *41*, 5918-5926, DOI: 10.1021/ie0202322.
- [28] Jiang, T.; Li, M.; Li, Y.; Xu, G.; Liu, C.; Eliasson, B.,

- Comparative investigation on the conversion of greenhouse gas using dielectric barrier discharge and corona discharge. *J. Tianjin University* **2002**, *35*, 19-22.
- [29] Ghorbanzadeh, A.; Lotfalipour, R.; Rezaei, S., Carbon dioxide reforming of methane at near room temperature in low energy pulsed plasma. *Int. J. Hydrogen Energy* **2009**, *34*, 293-298, DOI: 10.1016/j.ijhydene.2008.10.056.
- [30] Long, H.; Shang, S.; Tao, X.; Yin, Y.; Dai, X., CO<sub>2</sub> reforming of CH<sub>4</sub> by combination of cold plasma jet and Ni/γ-Al<sub>2</sub>O<sub>3</sub> catalyst. *Int. J. Hydrogen Energy* **2008**, *33*, 5510-5515, DOI: 10.1016/j.ijhydene.2008.05.026.
- [31] Lan, T.; Ran, Y.; Long, H.; Wang, Y.; Yin, Y., Experimental study on syngas production by carbon dioxide (CO<sub>2</sub>) reforming of methane (CH<sub>4</sub>) by plasma jet. *Nat. Gas Ind.* **2007**, *27*, 129-132.
- [32] Wang, B.; Yan, W.; Ge, W.; Duan, X. O., Kinetic model of the methane conversion into higher hydrocarbons with a dielectric barrier discharge microplasma reactor. *Chem. Eng. J.* **2013**, *234*, 354-360, DOI: 10.1016/j.cej.2013.08.052.
- [33] Yan, K.; van Heesch, E. J. M.; Pemen, A. J. M.; Huijbrechts, P. A. H. J., From chemical kinetics to streamer corona reactor and voltage pulse generator. *Plasma Chem. Plasma P.* **2001**, *21*, 107-137, DOI: 10.1023/A:1007045529652.
- [34] Rudolph, R.; Francke, K. P.; Miessner, H., Concentration dependence of VOC decomposition by dielectric barrier discharges. *Plasma Chem. Plasma P.* **2002**, *22*, 401-412, DOI: 10.1023/A:1015369100161.
- [35] Redolfi, M., PhD. Thesis of the University Paris XIII, **2007**.
- [36] Reddy, E. L.; Karuppiah, J.; Renken, A.; Kiwi-Minsker, L.; Subrahmanyam, C., Kinetics of the decomposition of hydrogen sulfide in a dielectric barrier discharge reactor. *Chem. Eng. Technol.* **2012**, *35*, 2030-2034, DOI: 10.1002/ceat.201200134.
- [37] Chiper, A. S.; Blin-Simiand, N.; Heninger, M.; Mestdagh, H.; Boissel, P.; Jorand, F.; Lemaire, J.; Leprovost, J.; Pasquiers, S.; Popa, G.; Postel, C., Detailed characterization of 2-heptanone conversion by dielectric barrier discharge in N<sub>2</sub> and N<sub>2</sub>/O<sub>2</sub> mixtures. *J. Phys. Chem. A* **2010**, *114*, 397-407, DOI: 10.1021/jp907295d.
- [38] Rosacha, L. A.; Korzekwa, R. A., Advanced oxidation, and reduction processes in the gas phase using non-thermal plasmas. *J. Adv. Oxid. Technol.* **1999**, *4*, 247-264.